STUDIES ON THE SPATIAL VARIABILITY OF GROUND MOTION FOR THE DESIGN OF EXTENDED STRUCTURES

E. Faccioli[1]

ABSTRACT

After outlining the causes of spatial variability in earthquake ground motions, paper illustrates some approaches to this problem developed in the analysis and design of actual or projected bridge structures. Collapse of the Cypress Viaduct in the 1989 Loma Prieta earthquake is considered first and, based on recent geotechnical data, it is shown that local differences of soil conditions do not easily explain why a part of the structure remained standing. Finally, an integrated approach for modelling both source and site effects in a large earthquake is presented , in connection with preliminary design studies for the projected crossing of the Messina Straits by a single-span suspension bridge.

INTRODUCTION

Quantifiying the spatial variability of vibratory ground motion is a problem typically encountered in the design of important bridges, and in many cases a challenging one. Variability of motion in horizontal direction can roughly be considered to depend on three main factors, namely:

1. finiteness of the seismic source;

2. material heterogeneities of the earth crust (at different length scales) and geometrical irregularities of the earth surface;

3. "propagation", or "wave-passage", effects arising from the finite apparent velocity at which seismic waves sweep across a site on the earth surface.

In the near-field of an extended seismic source ray paths extending from different portions of the ruptured fault will give rise to different ground motions at two points some distance apart, because of different azimuths, incidence angles,and scattering paths. Source finiteness generally reduces the spatial coherence of motion relative to that of a single point source. The variability caused by the source would persist even if the earth crust were a homogeneous half space, because of wave passage effects [16]. Spatial variability in the presence of an extended seismic source will be illustrated in more detail in a later section.

[1] Professor, Department of Structural Engineering, Technical University of Milan, Italy

Crustal heterogeneities influence the entire spectrum of seismic wavelengths : most significant are the irregularities in the surface geology and topography, capable of locally amplifying the ground motion at the natural frequencies of engineering structures. For instance, a change of stiffness in the uppermost 10 to 20 m of foundation soil may have locally enhanced the severity of ground shaking, and played a potentially important role in the collapse of the Cypress Street Viaduct, during the October 17, 1989 Loma Prieta earthquake in California. An evaluation of the seismic soil response variability for this case is presented in the next section.

In contrast to the previous situation, when no marked geological and topographic irregularities occur, seismic motions change smoothly in space over distances not exceeding few hundreds of m. Within this range the variations are due to small-size scatterers located in the site vicinity, and mostly affect the high frequencies. This is well illustrated by the data of the El Centro differential array in Fig. 1.

Dynamic analysis of bridge structures is commonly carried out by the standard response spectrum method, while the effect of spatially variable earthquake motion can be approximately accounted for by statically imposing some differential displacements at the supports. Only for bridges containing long spans are step-by-step analyses performed applying time-shifted, or multiple acceleration histories at the supports. Useful criteria for this purpose can be found in the recent French recommandations AFPS 90 [1].

In usual conditions the influence of spatial variability upon the maximum values of structural response is small, and can therefore be treated in simplified ways [3]. On the other hand, in the presence of significant geological/geotechnical discontinuities or marked topographical features, realistic models for predicting the variability should be used. The example of the Messina suspension bridge, discussed later, provides an interesting case history of the latter type.

THE CYPRESS VIADUCT COLLAPSE: DID HORIZONTAL VARIATION IN SEISMIC GROUND RESPONSE PLAY A ROLE ?

It was previously surmised that irregularities in local soil amplification may have contributed to the collapse of the Cypress Street Viaduct in the 1989 Loma Prieta earthquake. The following description taken from [6],summarizes the main characteristics of the structure. The Cypress Viaduct was a reinforced concrete structure, prestressed in part, carrying two levels of elevated roadway. The box girder roadway was supported by a series of 83 two-story bents, extending from Bent 29 through Bent 111. Box girders of multi-cell r.c. had spans varying from 21 to 27 m. As shown in Fig. 2, Bents 63 through 112 collapsed in the earthquake; only Bents 96 and 97 remained standing. No less than 11 bent types were used; however, 29 out of the 48 collapsed bents were of the same type (called B1) consisting of two portal frames, one mounted on top of the other. South of the collapsed portion, 24 out of 31 bents that remained standing were also of type B1; little damage was observed in Bents 32 through 48, while cracking in the concrete increased significantly from Bent 49 to Bent 62. The inadequate design criteria (the viaduct was designed and built in the early 1950s) made the structure highly susceptible to damage or collapse in a

strong earthquake. Studies by different specialists [6], show that the maximum elastic demands of base shear imposed by the earthquake on B1 bents were of the order of 40% of the weight, based on dynamic analyses. This exceeded by roughly a factor of 4 the static capacity for this nonductile structure, pointing to the conclusion that failure was inescapable. However, since the bent types do not change too much along most of the viaduct, it remains to be explained why a portion of the structure collapsed while that next to it remained standing.

A profile of the foundation soil along the viaduct (Fig. 3) discloses a sudden change in stratigraphy occurring near Bent 70 with the appearance of a 6-7 m thick surficial layer of bay mud, i.e. soft silty clay, concomitant with a dramatic change of pile length. The bents were in fact founded on groups of concrete filled pipe piles 30 cm in diameter,with the number of piles in the group varying from bent to bent . From Bent 34 through 71, the average pile length is about 4.5 m, while from Bent 72 through 111 the average length is about 15 m, with a jump in length of 9 m from Bent 71 to Bent 72. There is no evidence of failure of the foundation system.

A detailed description of soil stratigraphy is given by Rogers [11]. Geotechnical data obtained during construction were integrated by the end of 1990 with additional borings executed by the California Department of Transportation (Caltrans). Two of these, identified as B2 and B8 and located as shown in Fig.2, were drilled to more than 170 m depth, to encounter Franciscan bedrock (graywacke sandstone and shale). The soil profile at B2 and B8, displayed in Fig.4, shows a bedrock surface sloping gently to the N,in addition to some differences in stratigraphy between the two sites. Especially noticeable at B8 is the absence of the surficial sandy layer that can be seen at B2, and the presence instead of silty/clayey materials (bay mud).

Downhole geophysical surveys were carried out in both holes by two different techniques to determine accurate values of the S wave velocity ß;the recommended velocity models based on the combined results of the surveys are displayed in Fig. 4. The B2 profile,located in the portion of the Viaduct which remained standing, mainly differs from the B8 profile (located in the collapsed zone) because of the ß values of the topmost 23 m or so; the presence of the sand at B2, instead of the bay mud, corresponds to an increase in ß by over 50 percent. At first sight, this appears as a potential cause of differences in dynamic soil response at site B8 with respect to site B2.

The fundamental transverse vibration frequency of the bents was estimated by different authors to be 2.4-2.6 Hz. Hence, if local variations in soil amplification had an influence on structural response, at such frequencies (or somewhat lower ones, to account for structural degradation) we would expect to find higher response spectral ordinates for site B8.

Although no accelerograph recorded the Loma Prieta earthquake at the Cypress Viaduct site, a remarkable coherence of ground displacements has been found at the closest recording stations EMV,OHW and 2ST (ground floor) in the Oakland area, shown in Fig. 5, all located on deep soil sites within 2.5 km distance and roughly 80 km from the epicenter [6]. Since the collapsed section of the Viaduct lies close to the center of the triangle formed by the previous stations, the ground motion under such section should have been similar to that recorded at the three stations.

However, strong aftershocks recorded by portable seismographs on different soil conditions in the same area in the week following the main event show that on a bay mud site about 600 m W of the collapsed section of the freeway the ground motion was amplified with respect to an alluvium site E of the southern, uncollapsed portion characterized by essentially similar ground conditions [11].

In the main shock, the peak horizontal accelerations were 0.26 g at EMV (EW), 0.29 g at OHW (35°), and 0.24 g at 2ST (290°). The closest recording to Cypress on a rock outcrop was obtained at the YBI station, also shown in Fig. 5, with a peak value of 0.07 g. It is reminded that in the Bay area, within the 75 to 80 km range of epicentral distances, recorded peak accelerations on rock varied between a minimum of 0.06 g and a maximum of 0.11 g.

The soil profiles at B2 and B8 were modeled as 1D systems of plane layers, excited by the same acceleration history,i.e. the YBI 90° component; their seismic response was computed by a standard equivalent linear method [13] assuming a halfspace with ß = 520 m/s at depths of 91.5 and 119 m for B2 and B8, rispectively. Curves describing the variation of normalized shear modulus and damping for the different materials were taken from the literature [8]. The computed response spectra for 0.05 damping are illustrated in Fig. 6a for the YBI 90 ° input as recorded, and in Fig. 6b for the same input scaled to a peak acceleration of 0.11 g. The results fail to disclose any significant difference of spectral ordinates between B2 and B8 at periods of 0.4 to 0.5 s, corresponding to the fundamental frequencies of the bents. Even worse, the computed spectral ordinates are much lower than those of the average spectrum obtained from the observed motions at the three nearest stations of Fig. 5.

The possibility exists that the chosen input is not representative of bedrock motions at the Cypress site, which is not unlikely in view of the irregular geometry of the Franciscan basement under the Oakland area and the fact that Yerba Buena Island constitutes an isolated topographic high [11].These circumstances also suggest that 1D modeling of seismic soil response is inadequate, resulting in gross underprediction of the expected level of the spectral ordinates over a large range of periods, in agreement with other studies. It is not clear at this stage whether propagation of locally excited surface waves along the viaduct axis represents a realistic possibility.

A third possibility is to rule out any significant differences in site effects, and attribute the cause of the observed differences among distinct portions of the viaduct to structural factors, such as the jump in stiffness (and, hence, of vibration period) occuring across Bent 72 because of the sudden change in pile length [11].

EVALUATING THE VARIABILITY OF MOTION CAUSED BY A LARGE NEAR-FIELD EARTHQUAKE

Context

The preliminary design work for a suspension bridge across the Messina Straits, between Sicily and Calabria (Southern Italy), has been under way for some time, and is scheduled for completion in

late 1992. The realization of the crossing will call for a single span 3360 m in length and two main towers 390 m in height which would be the biggest ever built in a suspension bridge.

The Messina Straits lie in an area of high seismicity; in 1908 this was the seat of one of the most catastrophic earthquakes in Italian history (estimated M_s between 6.9 and 7.3) which caused 80.000 victims and widespread destruction in Messina and Reggio Calabria, the two cities facing each other across the Straits. A little over a century earlier, in 1783, the same two cities had been partially destroyed by the first in a sequence of strong earthquakes which devastated Calabria in a period of few months. Not surprisingly, an event comparable to that of 1908 was assumed as a design earthquake with a recurrence period of 2000 years and 0.64 g peak acceleration [5]. A near-field event with $M_s = 7+$ can generate long period motions as well as permanent displacements of particular significance for a structure with a fundamental period of vibration of about 33 sec. Even more important, the source effects of such an earthquake could combine with those of surficial geology to cause strong differences in ground motion on the two shores of the Straits. It was therefore felt that, as a support to the determination of design seismic actions, numerical modeling of both the source radiation and the site response had to be considered. A description of the approach to this problem and the illustration of some representative results is given in the following.

Source model and site model

Among the different reconstructions proposed for the causative fault of the 1908 earthquake [2], the one shown in Fig. 7 has been given priority in the analysis. Fig. 7b depicts the vertical cross-section A-A' through the trace of the crossing and also shows the seismic velocities and densities for the assumed crustal model; all these quantities pertain to the "source" model, i.e. to a model which calculates the seismic radiation from a finite source embedded in a layered medium. The values of this radiation, in the form of displacement time-histories at appropriate points, provide the input for the 2D "site" model, which incorporates the geological and topographic details of the cross-section under the bridge. The portion of site model lying between the two towers, labelled 1 and 5, corresponds to the hachured rectangle in Fig. 7b.

Since the free surface of the earth is included in the site model, there must be no free surface in the "source" model, and therefore the uppermost layer in Fig. 7b has infinite thickness. The source model calculations were performed [7] using the 3D method and computer program of Olson et al. [9], combined with a randomization of the rupture process [12]. The total rupture area is subdivided into smaller subfaults with random areas (but fixed aspect ratio), determined from an exponential distribution with prescribed mean value. Rupture propagates with a velocity stochastically varying in each subfault, which is further characterized by a ramp-like slip function with slope proportional to the rupture velocity and by a final slip amplitude. The overall seismic moment is constrained in the range 2.8×10^{19} - 11.2×10^{19} Nm, depending on the assumed M_s value for the 1908 event, the total rupture area being fixed at 750 km^2 . The estimated slip for the 1908 earthquake was about 1.5 m.

Even if the radiated spectrum has an upper band limitation at 2 Hz, the computational procedure is expensive. However, the randomization yields synthetic seismograms with a more realistic degree of complexity than a deterministic rupture. It can also provide many realizations of ground motion for a fixed earthquake size and location, which is convenient for obtaining statistical measures in engineering applications.

"Site" effects are introduced by: (a) taking as incident waves the "source" motions at appropriate interface points between the two models such as 2', 2,....4' in Fig. 7c, and (b) propagating such motions in a discrete 2D model of the zone of the crossing. The size of this model (approximately 5.6 x 0.7 km) is shown in Fig. 7c. The geological cross-section, given in Fig. 8, exhibits a graben-like structure, but none of the numerous normal faults cuts the uppermost layer of Holocene sediments. Several faults, especially on the Calabrian shore, must be regarded as geologically active, but only the cumulative slip over a period of the order of one million years has been estimated. The hazard posed by surface rupturing of a given fault during a single earthquake varies considerably with location, but remains moderate (few tens of cm, at most, for the 2000 years event).

Deep reflection surveys were used to resolve the geological structure at depths larger than about 200 m, supported by two preexisting deep drillings near the projected sites of the bridge towers. Such surveys also provided values of the longitudinal seismic velocity, α , of the main formations. On land, at the tower and anchor block sites on both shores, α and ß values were measured by cross-hole tests in at least two pairs of adjacent borings. Fig. 9 shows the dynamic characteristics of the Sicily foundation to be those of a moderately stiff, deep deposit, with the Holocene materials reaching about 70 m depth and overlying the Messina gravels of Upper Pleistocene. On the other hand, the Calabria tower will rest on a much stiffer site. Dashed lines in Fig. 9 give the low-strain values assumed on the corresponding vertical of the "site" model, which has a grid spacing of 25 m. Figs. 8 and 9 illustrate the stratigraphic differences between the two shores, especially evident in the elevation of the "Pezzo conglomerate" formation which has values of $ß \geq$ 750 m/s and represents the seismic "bedrock" for the area. Also, the slope of the sea bottom in the vicinity of the Calabria foundation is much steeper than on the Sicily side.

Values of ß for the offshore portions of the model, and for land portions deeper than 100 m were derived from values and a ratio $\alpha / ß = \sqrt{3}$. Fig. 10 illustrates, with simplifications, the discretized model derived from the cross-section of Fig. 8. The 2D numerical wave propagation in this model was limited for simplicity to SH motion, and was performed by the pseudospectral method. While its characteristics and performance are described elsewhere [4], the program WAVE2D was specially developed for this purpose, taking full advantage of the resources of vector computers.

The analysis obviously requires that the incident motion be normal to the plane of the model. Owing to the proximity and dimensions of the seismic source, the incident waveforms change smoothly in space but the main pulse in them remains identifiable over the distances of interest for the site model, as shown by the seismograms at points 2 and 4 in Fig. 11. The apparent horizontal velocity of the main pulse between a pair of interface points (4'-4, 4-3,...see Fig. 7c) can thus be

estimated, and the incident waveform at any intermediate position reconstructed by simple linear interpolation. In this way, at each grid point on the base of the site model a different motion is prescribed and non-plane waves can be treated, limiting the expensive calculations of the incident field by the source model to a small number of points.

The discretized grid step h = 25 m results from a requirement of the pseudospectral method to avoid aliasing, namely that the frequency band to be propagated in a homogeneous medium be limited by the value $f_{max} \leq ß/2h$. In heterogeneous media, $ß_{min}$ must be replaced by $ß_{min}$ and the factor 2 by a value between 3 and 4. The motions generated by the present source model have an upper cutoff at 2 Hz, while $ß_{min}$ = 250 m/s. In the numerical analyses $ß_{min}$ was reduced to 200 m/s, to account for the strain levels induced by earthquake motion, and the ß values of the underlying materials (up to the Pezzo conglomerate) were likewise reduced by about 25 %. A spatially uniform internal dissipation was introduced, such as to give a material damping coefficient of 0.012 at 2 Hz; this corresponds to a quality factor linearly varying with frequency, i.e. Q = 20 f.

Results

Fig. 11 illustrates, for just one synthetic earthquake , the variability in surface response caused by site conditions along the crossing. The peak amplification ratio is about 4.0 along the vertical of both Calabria and Sicily towers, while the dominant frequency of motion at these sites change from 0.6 Hz to about 1.0 Hz. Significant duration does not exceed about 10 sec on both sites. The calculated a_{max} in this example ranges from 0.5 g (Sicily shore) to about 1 g (Calabria shore),not unrealistic for sites in the near field of an M_S 7.0 earthquake, as suggested by the 0.64 g value recorded during the Loma Prieta event. Note that a design value of 0.64 g was assumed for a recurrence period of 2000 years. 2D site effects show up in the character of motion after the strong initial peaks, which are caused by vertically propagating waves; the lower peaks that follow, and the coda, are in fact mostly the result of horizontally propagating surface waves. These are mostly confined within the uppermost gravelly formation and are strongly affected by internal dissipation, so that a fast amplitude decay occurs over relatively short distances, even with small damping. Given the length scales of the irregularities and the ß values at play, the periods of horizontally propagating waves do not exceed a few seconds. The corresponding wavelengths are clearly visibile in the "snapshot" of the synthetic acceleration field shown in Fig. 12.

Finally, the response spectra of calculated motions at the tower sites are displayed in Figs. 13 together with the input spectra at interface points on the corresponding vertical. The period range of maximum amplifications lies between 0.5 sec and 1.0 sec at the Calabria site, but it extends to larger periods at the softer Sicily site.

Additional simulations of the type just described are being performed, corresponding to other realizations of the rupture process at the source, to obtain statistically representative results. The example of Figs. 7 - 13, however, is well representative of the extent to which calculated surface motions can be affected both by the seismic source and by site conditions. It appears that the latter

factor exerts in this case a dominant influence on spatial variability of surface motion. Simplified response calculations by 1D models, not shown here, provide acceptable estimates of peak ground motion values, but underestimate the significant duration of motion and the spectral ordinates in some frequency intervals.

CONCLUSIONS

The main sources of spatial variability in earthquake ground motion over the length scales of interest for multi-support structures, especially long bridges, seem to be the irregularities in near-surface geology and topography. The variability due to the proximity of an extended earthquake source, although not very significant per se, may combine with site effects to produce strong localized anomalies. Stochastic characterizations of spatial variability and associated methods for generating artificial seismograms are nowadays the object of increasing interest, see e.g. [14]. Their usefulness, however, is partly open to question, as they are mainly applicable to standard site conditions, i.e. when the leading cause of spatial variability lies in wave passage effects, or in moderate scattering, which mostly have a small influence on maximum structural response. On the other hand, the influence of geological and topographic irregularities is more marked and complex, and it poses a stronger need for realistic predictions of ground motion, either by appropriate observational data or by direct physical modeling of the earthquake response at the sites of interest.

Although the example of the Messina bridge illustrated here required large-scale numerical modeling, other practical cases of importance can be approached by means of simpler tools, e.g. closed-form solutions for elementary 2D geometries [4]. More research focused on such simplified methods, as well as a wider diffusion of the existing ones among designers and analysts, would be desirable.

ACKNOWLEDGMENTS

We are grateful to Prof. James Mitchell, who timely sent us technical material and newly released soil data for the Cypress Viaduct site. The development of computer program WAVE2D was made possible by the cooperation of Maurizio Fontana at Studio Geotecnico Italiano. Stefano Bacci, of the same organization, prepared all figures. Thanks are also due to Paola Nava, who typed the manuscript. Finally, the permission by Stretto di Messina Spa to make use of the material in Figs. 7 to 13, is gratefully acknowledged. This research was partially sponsored by Italy's National Research Council (C.N.R.- Gruppo Nazionale Difesa Terremoti) under Contract No.89.01983.54.

REFERENCES

1. Association Francaise du Genie Parasismique, Recommandations AFPS 90, Presses Ponts et Chaussées, Paris, 1990.

2. Boschi E., Pantosti D., and Valensise G.,Modello di sorgente per il terremoto di Messina del 1908 ed evoluzione recente dell'area dello Stretto, Atti VIII Convegno Gruppo Naz. Geofis. Terra Solida C.N.R., Roma 1989.

3. Duarte R., Spatial Variability of the Earthquake Motion, Appendix D to Part 2 (Bridges) of Eurocode 8, Draft Manuscript, 1990.

4. Faccioli E., Seismic Amplification in the Presence of Geological and Topographic Irregularities, Proc. 2 nd Intern. Conf. Recent Advances in Geotechnical Earthquake Engineering and Soil Dynamics, St. Louis, Missouri, vol . II, pp. 1779-1797, March 1991.

5. Grandori G., Castiglioni A., Petrini V. e Urbano C., Studio del terremoto di progetto per l'opera di attraversamento dello Stretto, Report to Stretto di Messina SpA, 1985.

6. Housner G.(Chairman), Competing Against Time. Report to Governor George Deukmejian, from The Governor's Board of Inquiry on the 1989 Loma Prieta Earthquake, State of California, Office of Planning and Research, 1990.

7. ISMES, Modellazione " near-field " di sorgenti sismiche nei pressi dello Stretto di Messina. Relazione sulle analisi stocastiche, for Stretto di Messina S.p.A., Doc. RAT-DMM-4884, Bergamo, Italy, 1989.

8. Lodde P. "Dynamic response of San Francisco bay mud", M. Sc. Thesis, University of Texas, Austin, 1982.

9. Olson A., Orcutt J. and Frazier G., The Discrete Wavenumber/Finite Element Method for Synthethic Seismograms, Geophys. J.R. astr. Soc. 77, pp. 421-460, 1984.

10. Redpath B., Borehole Velocity Surveys at the Embarcadero in San Francisco and the Cypress Structure in Oakland, Report to California Department of Transportation under Contract No. 65M598, 1990.

11. Rogers J., "Site stratigraphy and its effects on soil amplification in the Greater Oakland area during the October 17, 1989 Loma Prieta earthquake", Proc. 2nd Intern. Conf. Recent Advances in Geotechnical Earthquake Engineering and Soil Dynamics, St. Louis, Missouri, Preprint Vol.pp 179-211,March 1991.

12. Savy J.B., A Geophysical Model of Strong Motion for Large Ensemble Generation, Res. Rep. R81-6, Dept.of Civ. Engn., M.I.T., Cambridge, Massachusetts, 1981.

13. Schnabel P., Lysmer J. and Seed H., SHAKE-A Computer Program for Earthquake Response Analysis of Horizontally Layered Sites, Report 72-12, Earthq. Engn.Res. Center, University of California, Berkeley, California, 1982.

14. Shinozuka M., State-of-the-Art Report. Engineering Modeling of Ground Motion, Proc. 9 th WCEE, Tokyo-Kyoto, VIII, pp. 51-62, 1988.

15. Smith S., Ehrenberg J. and Hernandez E., Analysis of the El Centro Differential Array for the 1979 Imperial Valley Earthquake, Bull. Seismol. Soc. Am. 72, pp. 237-258, 1982.

16. Somerville P., Mc Laren J., Saikia C. and Helmberger D., Site- specific Estimation of Spatial Incoherence of Strong Ground Motion, in L. Von Thun (ed.), Earthquake Engineering and Soil Dynamics II - Recent Advances in Ground-Motion Evaluation, Geotechnical Special Publ. n.20, ASCE, New York,pp. 188-202, 1988.

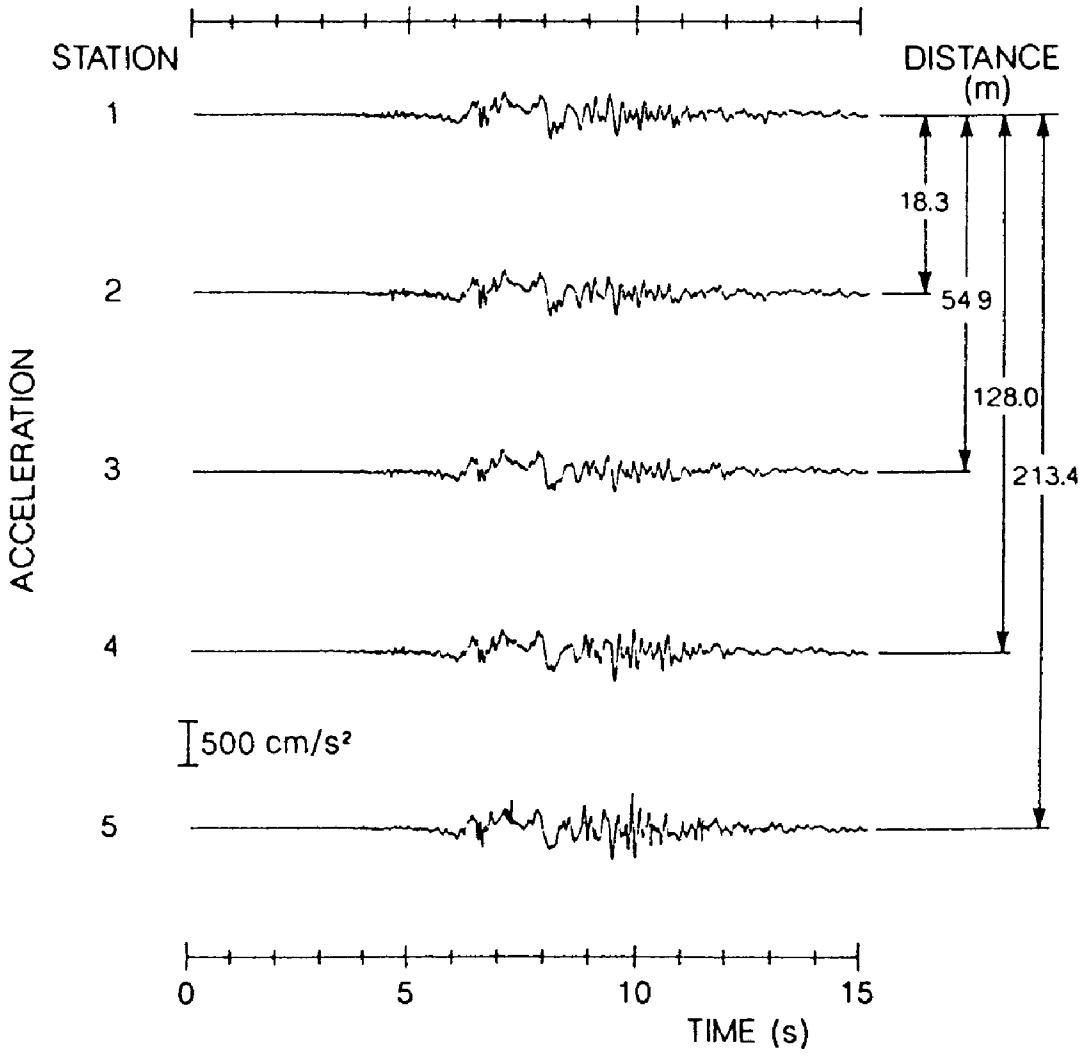

FIGURE 1. EW acceleration components digitally recorded at stations of El Centro differential array during the M_L 6.6 Imperial Valley, California earthquake of 15 10 79 [15]

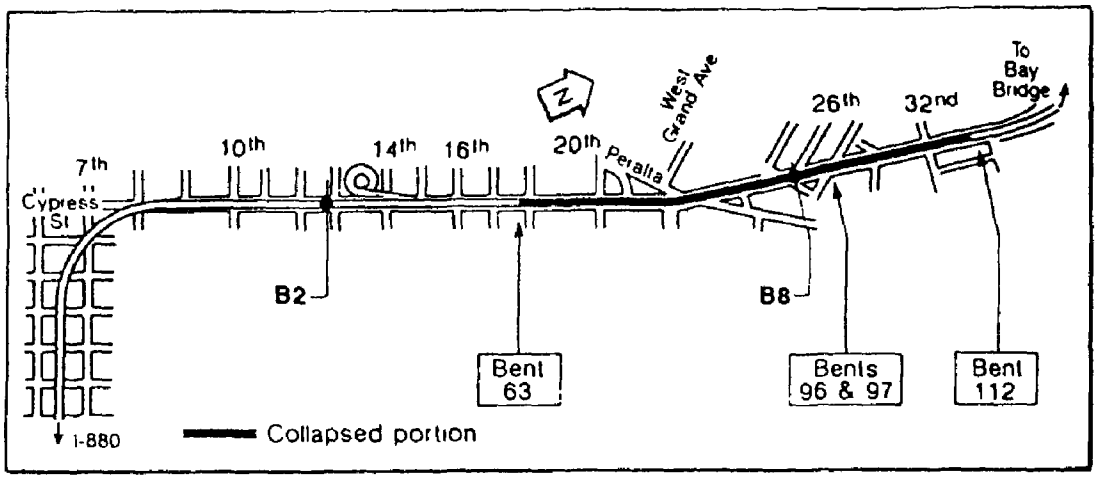

FIGURE 2. Plan of Cypress Viaduct in West Oakland, California, showing the limits of the collapsed portion and the location of deep borings B2 and B8 [6]

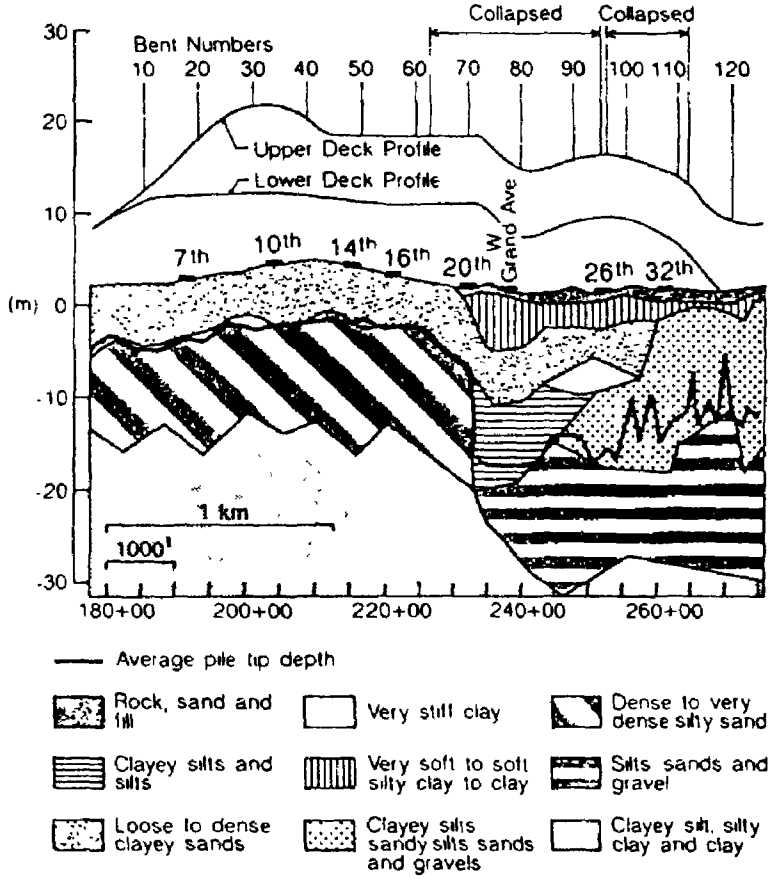

FIGURE 3. Soil profile of Cypress Viaduct based on Caltrans boring information from 1953-1990 [6]

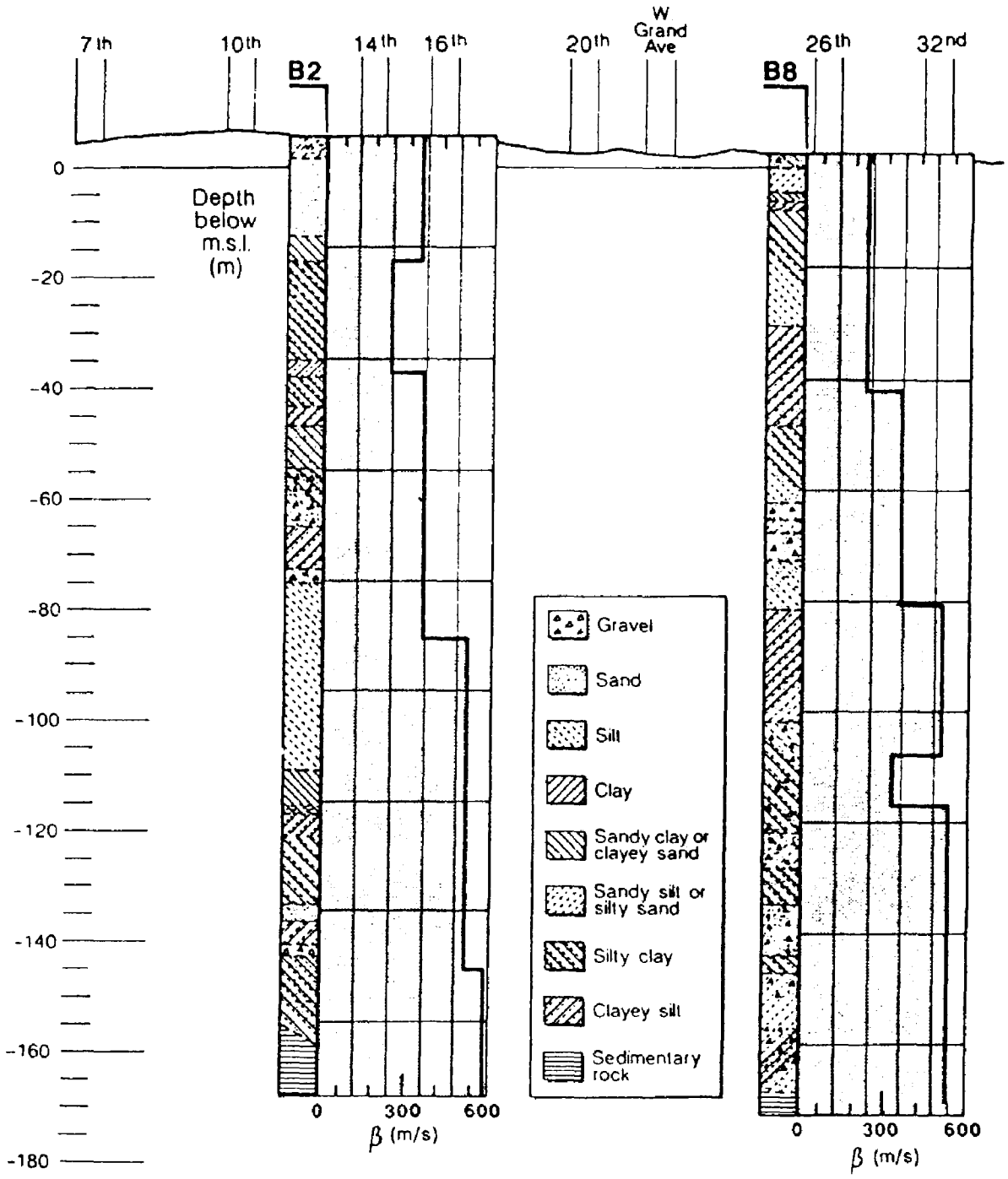

FIGURE 4. Profile of soil (Caltrans data, 1990) and of S wave velocity β [10] at deep borings B2 and B8 drilled along the Cypress Viaduct alignment, see Fig.2 .

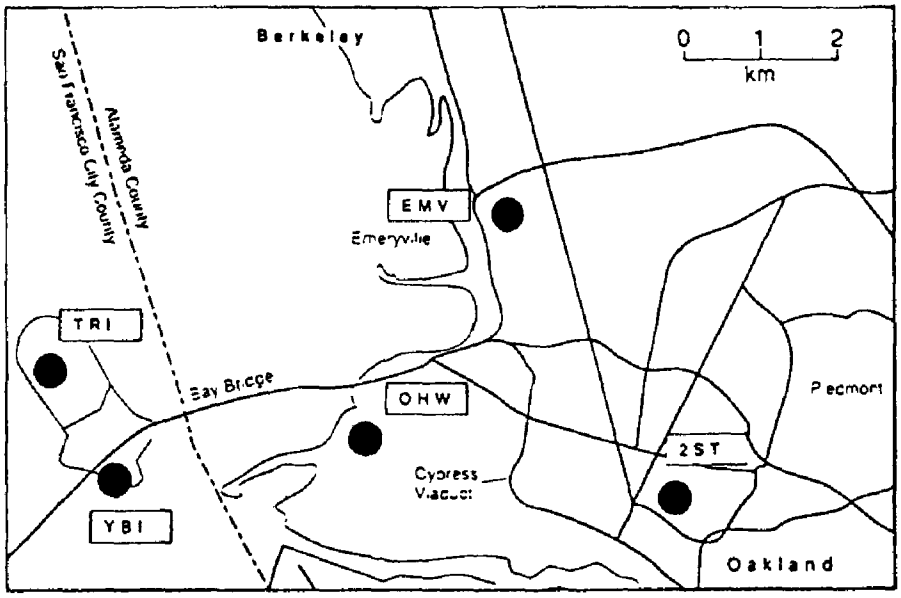

FIGURE 5. Map showing the location of selected strong-motion recording sites in the San Francisco - Oakland area . Emeryville (EMV), Oakland Outer Harbor Wharf (OHW) two-story building in Oakland (2ST), Treasure Island (TRi), Yerba Buena Island (YBI). After [6].

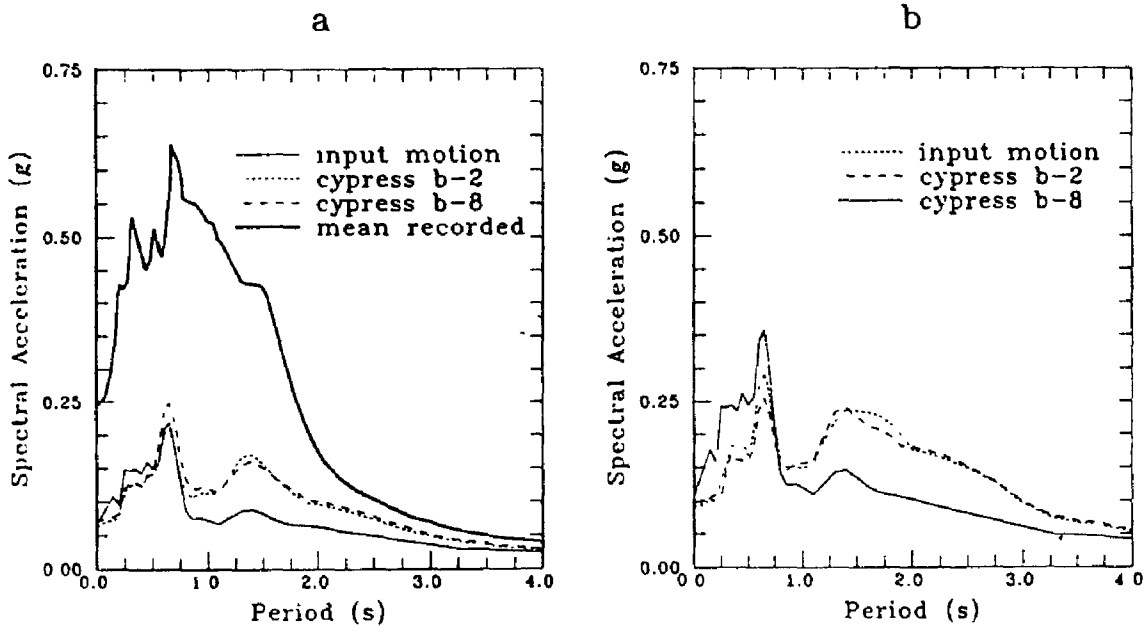

FIGURE 6. Computed response spectra (0 05 damping) for Cypress Viaduct sites using as input motion the YBI 90° acceleration component, (a) not scaled, and (b) scaled to 0 11g peak acceleration

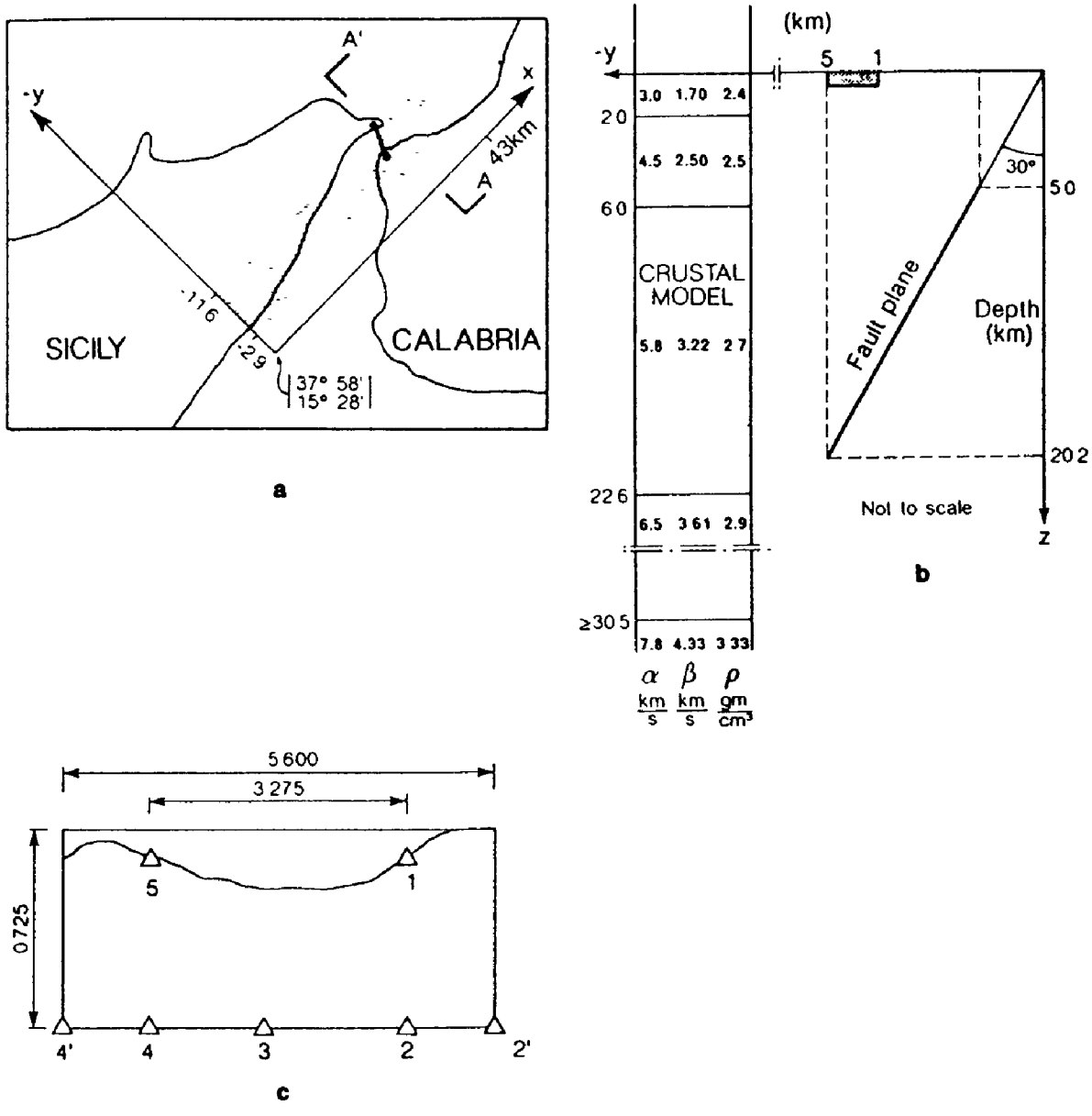

FIGURE 7. (a) Surface projection of causative fault of 1908 earthquake, (b) Cross-section A-A' of fault plane with assumed crustal model, and position of "site" model (hachured rectangle) shown in (c), (c) dimensions of "site" model in km, with triangles showing interface and surface points

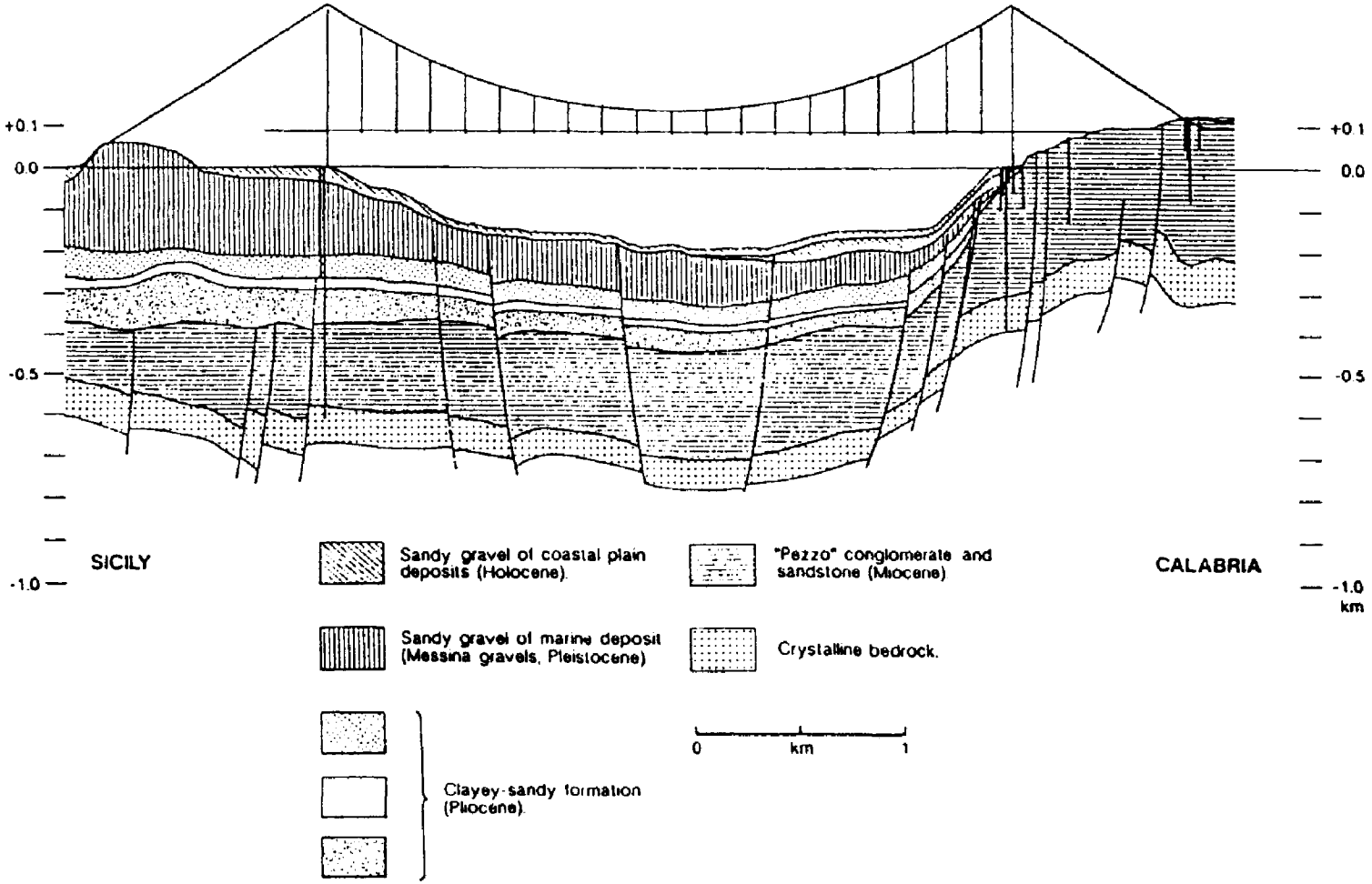

FIGURE 8. Stratigraphic cross-section of proposed Messina Straits crossing.

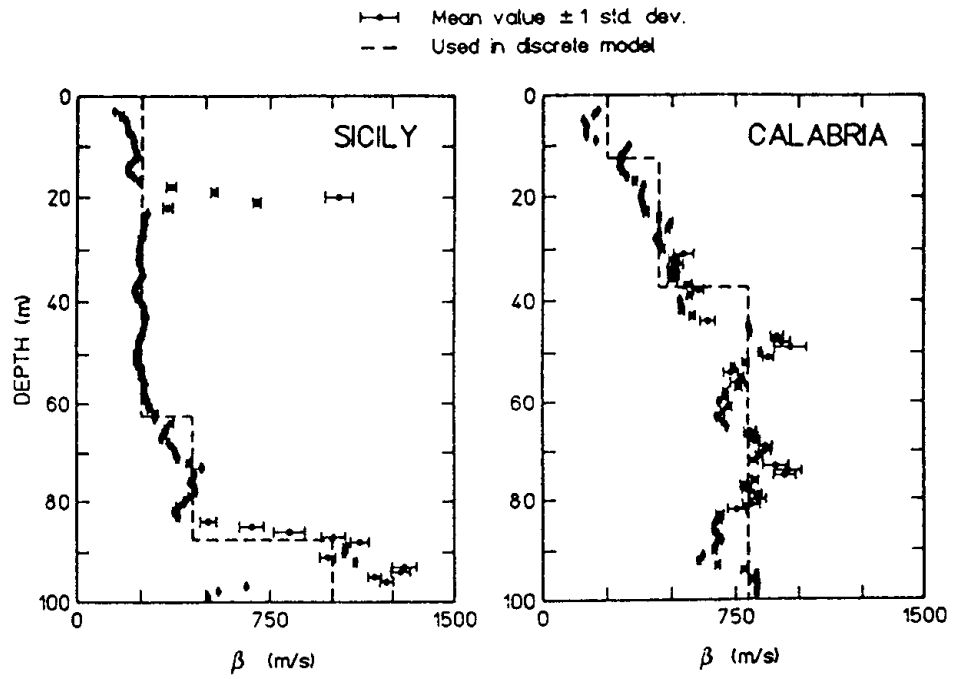

FIGURE 9. S wave velocity profiles at tower sites, from cross-hole surveys.

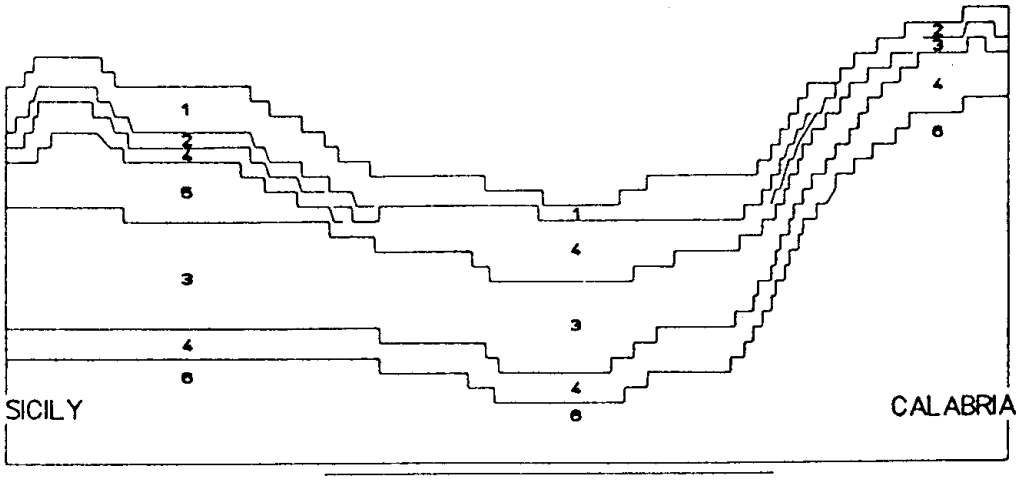

MATERIAL	β (m/s)	W (kN/m³)
1	250	19
2	450	19
3	800	20
4	1000	20
5	1350	20
6	1700	24

FIGURE 10. Geometry and material properties of 2D discrete model.

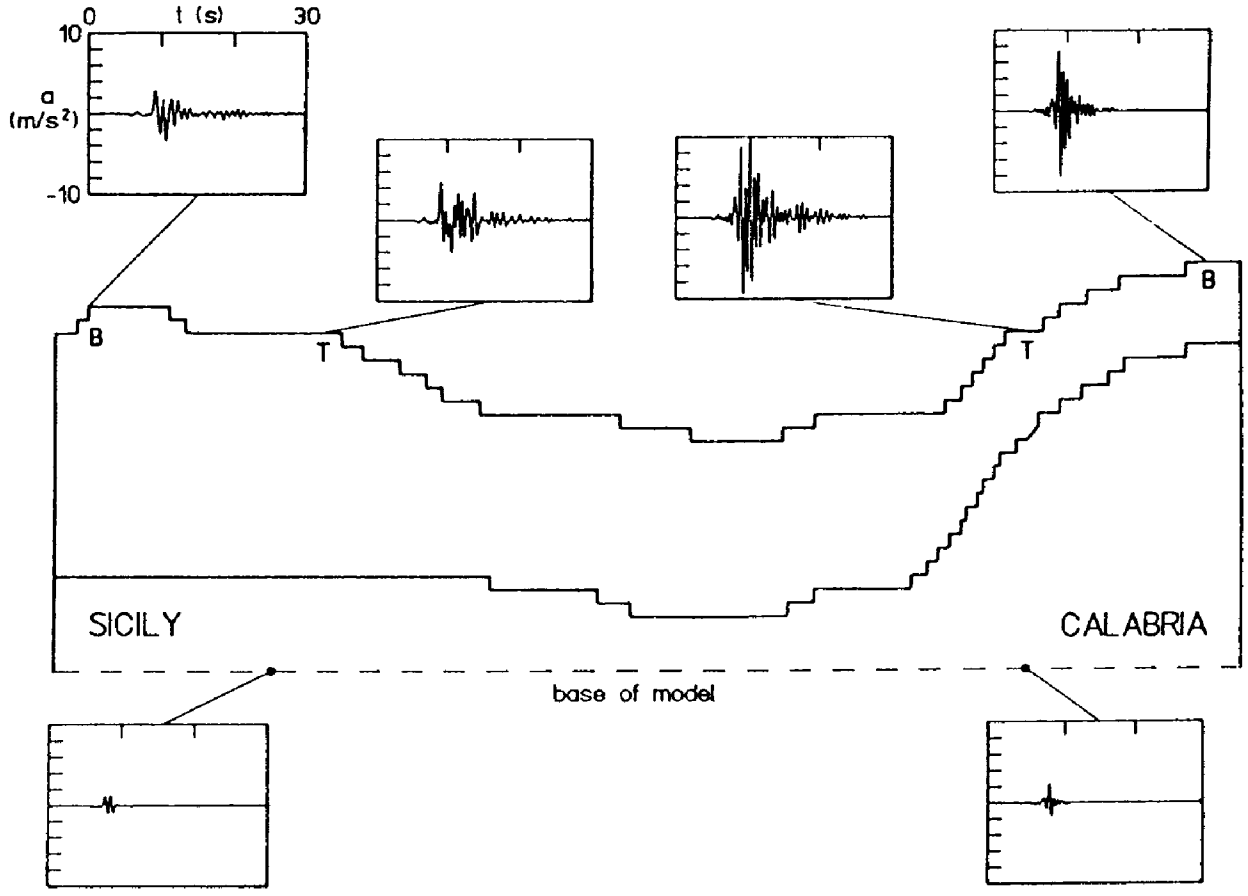

FIGURE 11. Calculated acceleration response to one input earthquake, T=tower, B=anchor block.

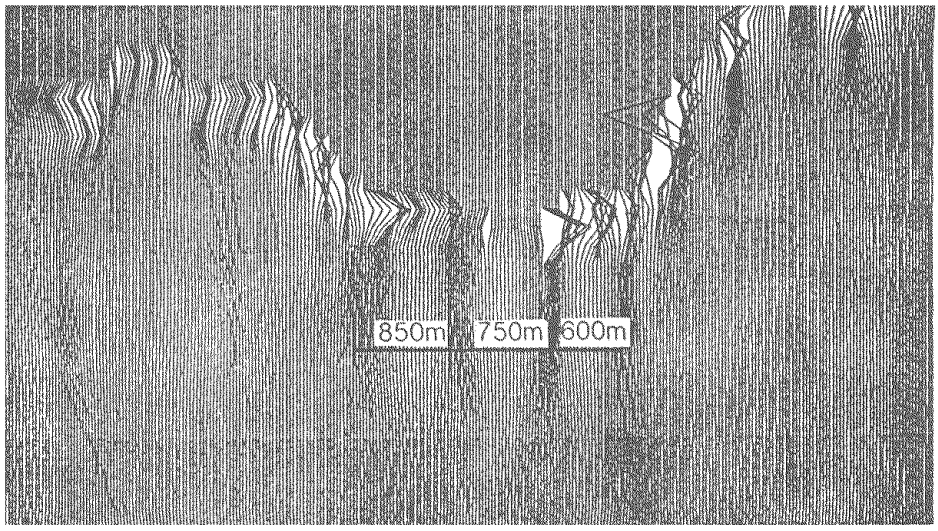

FIGURE 12. "Snapshot" of the synthetic acceleration field generated at instant t=11sec by the input earthquake of Fig.11. Indicated are also the apparent lengths (in m) of horizontally propagating waves.

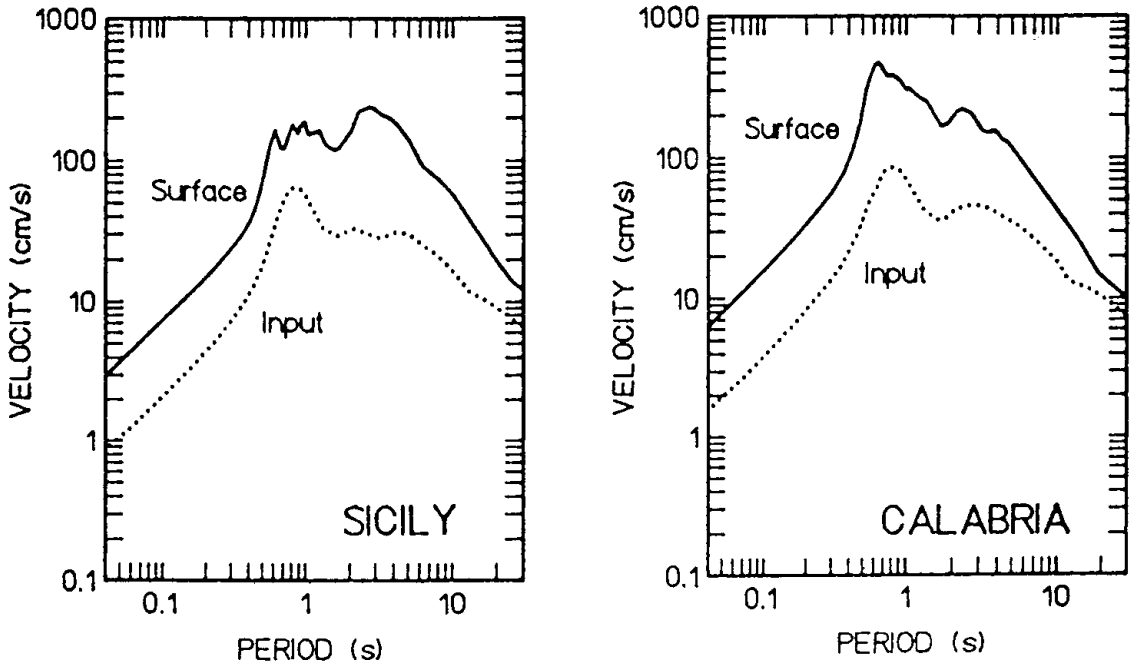

FIGURE 13. Elastic response spectra (0.05 damping) calculated at the tower sites from the synthetic motions of Fig.11.